Fabrication of SnO₂ three dimentional complex microcrystal chains by carbothermal reduction method

Neha Bhardwaj, Satyabrata Mohapatra*

School of Basic and Applied Sciences, Guru Gobind Singh Indraprastha University, Dwarka, New Delhi 110078, India

*Corresponding author. Tel: (+91) 11 25302414; E-mail: smiuac@gmail.com

ABSTRACT

Three dimensional (3D) complex microcrystal chains of SnO₂ have been fabricated by simple carbothermal reduction based vapour deposition method. The structural and optical properties of the as-synthesized materials were well characterized by field emission scanning electron microscopy (FESEM) with energy dispersive X-ray spectroscopy, X-ray diffraction (XRD), Raman spectroscopy and photoluminescence spectroscopy. FESEM studies revealed the formation of 3D complex chains of microcrystals of SnO₂ of varying shape and size. The SnO₂ microcrystals have been found to be inter-connected through oriented attachment, leading to the formation of 3D complex chains of microcrystals. XRD studies showed the presence of SnO₂ and Sn in the synthesized material. Photoluminescence studies on SnO₂ microcrystal chains revealed peaks at 361, 407, 438 and 465 nm. A tentative mechanism of formation of the 3D complex chains of SnO₂ microcrystals is proposed. These SnO₂ microcrystal chains have potential applications as building blocks in novel functional devices. Copyright © 2015 VBRI press.

Keywords: SnO₂; microcrystals; oriented attachment; microchains.

Satyabrata Mohapatra is working as Assistant Professor of Nanoscience and Technology at School of Basic and Applied Sciences, Guru Gobind Singh Indraprastha University, New Delhi, India. His current research involves synthesis and ion beam engineering of multifunctional hybrid nanostructures and plasmonic nanocomposites for the development of ultra-sensitive chemical and biosensors, gas sensors, and highly efficient photocatalysts.

Introduction

Fabrication of architectures of micro- and nanostructures of semiconductors is one of the major challenges for development of novel functional devices. Nanostructured semiconductors exhibit shape and size-dependent unique optical and electronic properties, which opens up possibilities for diverse technological applications. Tin oxide (SnO₂), an n-type wide band gap semiconductor (E_g = 3.6 eV), has attracted significant attention as a promising material for a wide range of applications including gas sensors, solar cells, catalysts and lithium ion batteries [1-

8]. Different physical and chemical methods have been used to synthesize SnO₂ nanostructures with different morphologies *viz.*, nanodisks [9], nanosheets [10], nanobelts [11], nanorods [12], and nanowires [13]. However, it is still challenging to fabricate 3D complex SnO₂ micro- and nanostructures with desired shape and crystallinity.

Oriented attachment (OA) is a special kind of aggregation which is found to be a promising route to the formation of complex shaped nanostructures [14-16]. Formation of nanostructures viz., TiO₂ nanocrystals [17, 18], ZnS nanoparticles [19], ZnO nanorods [20] and CdTe nanowires [21] have been explained well on the basis of OA mechanism. The OA mechanism relies on coalescence and self-organization of adjacent nanocrystals which generally occur upon collision between nanocrystals with mutual orientation. Lee et al. [22] reported the formation of dispersed anisotropic nanostructures by OA mechanism, under hydrothermal conditions. The OA mechanism has been successfully used to explain the growth of SnO₂ nanocrystals [23]. Zhuang *et al.* [24] reported the growth of SnO₂ nanoparticles by a hydrothermal process involving the OA mechanism. It is seen that most of the fabricated nanostructures formed by OA are generally synthesized by hydrothermal methods [25, 26]. Li *et al.* [27] reported the fabrication of 3D complex ZnO microcrystals in vapor

phase under catalyst free conditions and explained the intergrowth of ZnO microcrystals by OA of well-defined ZnO microcrystals. Consequently, the ZnO microcrystals joined together by a specific rule leading to 3D complex chain-like structures. The sufficient thermal energy in the system and the continual impacts among ZnO microcrystals provided an environment in which the intergrowth of microcrystals took place similar to that in solutions.

In this paper, we demonstrate a simple procedure to fabricate 3D complex chains of SnO_2 microcrystals using carbothermal reduction based vapor deposition method. 3D complex chains of SnO_2 microstructures consisting of inter-connected SnO_2 microcrystals have been synthesized and their structural and optical properties have been studied. A tentative mechanism underlying the formation of the 3D complex chains of SnO_2 microcrystal is proposed.

Experimental

Materials

Tin oxide (SnO_2) and graphite powders were used as starting materials. Tin oxide powder was purchased from Merck, Germany and graphite powder was brought from CDH, India. Silver (metal) powder with 99.9% purity was purchased from Loba Chemie, India. All reagents were of analytical grade and used as received.

Method

The synthesis of SnO_2 microcrystal chains by carbothermal reduction based vapor deposition was carried out using a horizontal tube furnace with gas flow systems. Briefly, 1:1 mixture of tin oxide and graphite powders along with 1 % Ag was thoroughly mixed and pelletized. The pellet, on an alumina boat, was kept in the centre of a one side open-ended quartz tube and placed within the horizontal tube furnace. Si (111) substrates with native oxide were placed in a downstream position from the source material within the inner quartz tube at a distance of 8-10 cm from the source material. The source material was heated to 1050^oC for 30 minutes under Ar flow, following which the furnace was allowed to slowly cool down to room temperature. X-ray diffraction (XRD) studies were carried out using Panalytical X'pert Pro diffractometer with Cu K_α radiation (λ = 0.1542 nm). Field emission scanning electron microscopy (FESEM) and energy dispersive X-ray spectroscopy (EDX) studies on the samples were carried out. Raman spectra are recorded by Horiba Jobin Yvon LabRam using a spot size of 1 µm and a wavelength of 488 nm. Photoluminescence (PL) studies were carried out using an excitation wavelength of 325 nm at room temperature.

Results and discussion

Fig. 1 shows the FESEM images revealing the microstructure of the as-synthesized sample. Formation of microcrystals of varying shape and size and 3D complex chains of microcrystals were observed, as shown in **Fig. 1 (a-d)**. The magnified views of single chains of microcrystals are shown in **Fig. 1 (c-d)**, which clearly show the presence of 3D complex chains of microcrystals. These chains are made up of microcrystals connected in a special fashion with facets attached. Different types of 3D complex

chains of microcrystals were observed. In addition to these microcrystals of varying shape and size and 3D complex chains of microcrystals, very few nanowires were also observed. The observed formation of 3D complex chains of microcrystals of SnO_2 is really interesting.
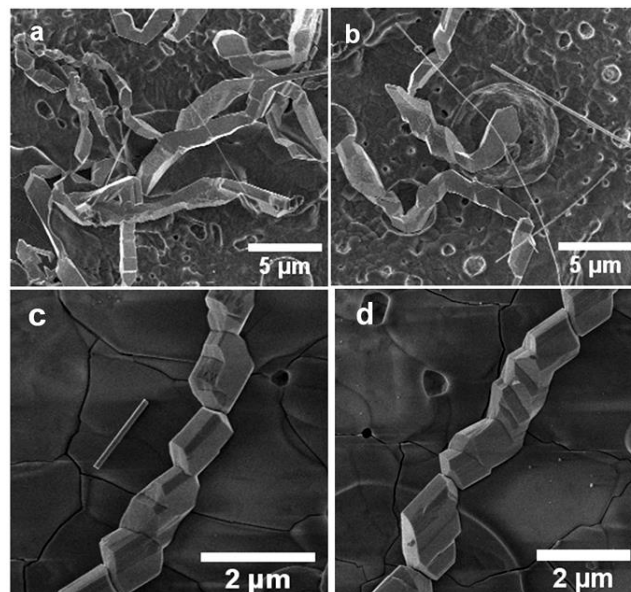
Fig. 1. **(a-b)** FESEM images of as-synthesized sample showing 3D complex chains of SnO_2 microcrystals, **(c-d)** magnified views of 3D complex chains of SnO_2 microcrystals.

The crystal structure of as-synthesized sample was characterized by XRD. **Fig. 2** shows the XRD pattern of the as-synthesised sample with microcrystal chains. The observed peaks are well indexed to the tetragonal structure of Sn and orthorhombic structure of SnO_2 in agreement with the standard data JCPDS 86-2265 and JCPDS 78-1063, respectively. No other peak corresponding to Ag, Ag_2O, Ag-Sn alloy or any other impurities was observed.
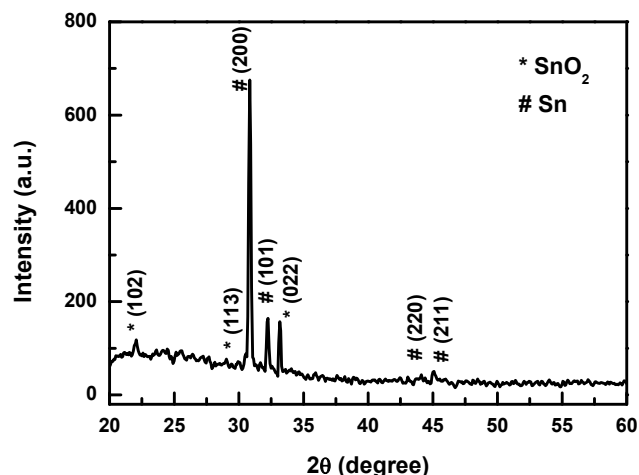
Fig. 2. XRD pattern of as-synthesized sample with 3D complex chains of SnO_2 microcrystals.

Fig. 3 shows the micro-Raman spectra of as-synthesized sample with 3D complex chains of microcrystals. The peaks at 396, 623, 792 and 124 cm^{-1} are assigned to A_{2g}, A_{1g}, B_{2g} and B_{1g} vibrational modes of SnO_2, respectively **[28-30]**. The modes A_{1g} and B_{2g} are

related to the expansion and contraction vibration modes of Sn-O bonds. In addition to the fundamental modes, two modes at 301 and 692 cm^{-1} are also detected. Sun et al. [31] have reported similar modes and ascribed them to infrared active E_u(3)TO and A_{2u}LO modes, respectively. Dieguez et al. [32] have attributed the bands between 475 cm^{-1} and 775 cm^{-1} to disorder activated surface modes. The Raman peak at 432 cm^{-1} is a consequence of surface disorder [29]. The observed peak at 520 cm^{-1} is from the Si substrate. Besides the various SnO$_2$ modes observed, there is one peak at 107 cm^{-1} which is ascribed to B_{1g} mode of SnO [33].
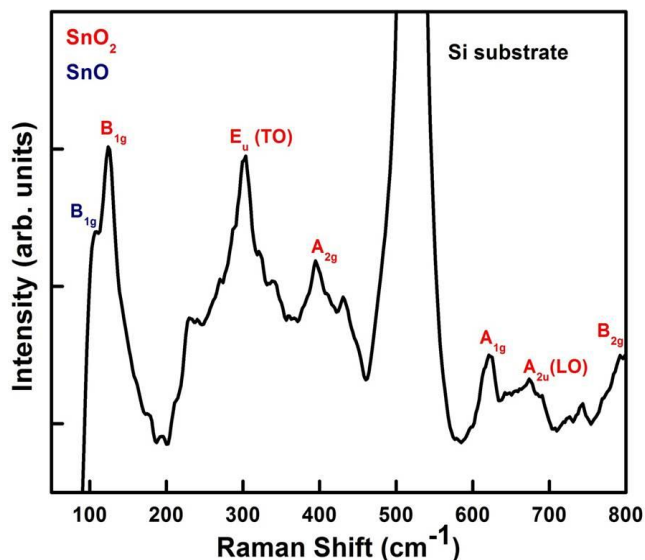
Fig. 3. Raman spectrum from 3D complex chains of SnO$_2$ microcrystals.

Fig. 4 shows the room temperature PL spectrum for the sample with 3D complex chains of SnO$_2$ microcrystals. The PL spectrum consists of peaks at 361, 407, 438 and 465 nm. Luo et al. [34] have shown that the UV emission from SnO$_2$ is due to near band edge (NBE) emission. In our case, the peak at 361 nm is attributed to NBE emission from SnO$_2$ microcrystals. The peaks at 407 and 438 nm are attributed to doubly ionized oxygen vacancies (V_O^{++}) [35].
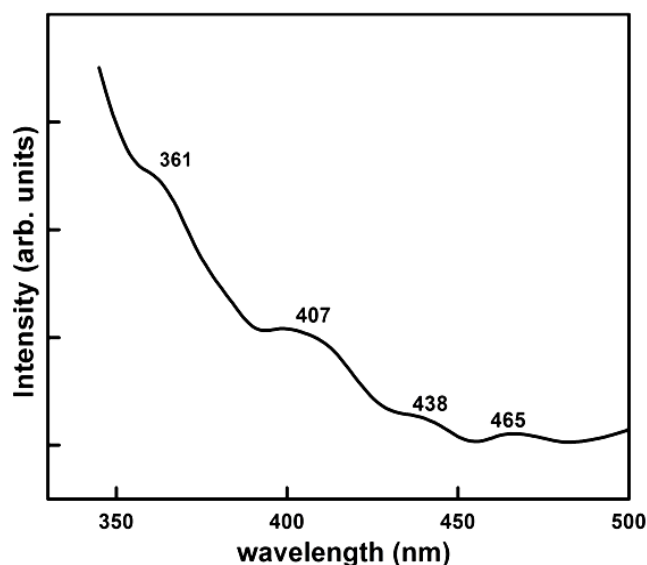
Fig. 4. Room temperature PL spectrum from sample with 3D complex chains of SnO$_2$ microcrystals.

The recombination of surface trapped hole with electron at the deep trap level (V_O^+) forms a doubly ionized oxygen vacancy centre (V_O^{++}). Kar et al. [36] have proposed a mechanism for defect related luminescence properties of SnO$_2$ nanostructures and showed that the defect emissions are produced when electrons from the conduction band recombine with the holes at (V_O^{++}) centres. The peak at 465 nm is attributed to electron transition mediated by defect levels within the band gap due to oxygen vacancies.
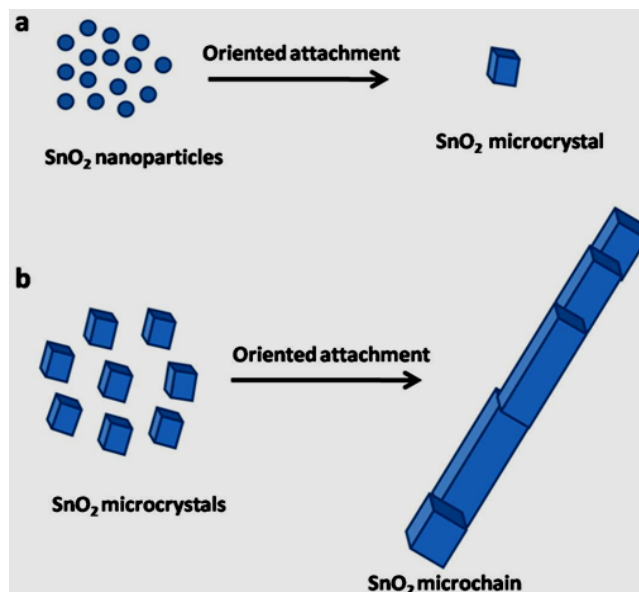
Fig. 5. Schematic diagrams showing mechanism of formation of 3D complex chains of SnO$_2$ microcrystals.

Understanding of the mechanisms underlying the growth of SnO$_2$ microcrystals and their inter-connected growth leading to 3D complex chains of microcrystals in an inert environment is very interesting. Penn and Banfield [14] explained the formation of micro-chain like structures of TiO$_2$ using the OA mechanism. The mechanism underlying the formation of 3D complex chains of microcrystals of SnO$_2$ is depicted as a schematic diagram shown in **Fig. 5**. The processes involving the formation mechanism can be summarized as: (i) formation of SnO$_2$ microcrystals due to oriented attachment of SnO$_2$ nanoparticles (**Fig. 5 (a)**) and (ii) oriented attachment of SnO$_2$ microcrystals resulting in 3D complex chains of SnO$_2$ microcrystals. Similar phenomenon has been reported in the formation of ZnO microcrystals via OA mechanism [27]. In our case, the observed 3D complex chains of microcrystals of SnO$_2$ are formed mainly due to the OA process, as shown in **Fig. 5 (b)**. The key characteristic of the OA process is that crystals grow along a crystallographically specific direction. Thermodynamically, the combination of the building blocks mainly relies on two factors, *viz.* the surface energies and the extent of lattice matching of the attached surfaces. It has been found that only the facets that have the same or similar surface energies and crystal orientations can attach together [14-16]. In our case, when the source material containing SnO$_2$, graphite and Ag was heated to 1050°C, carbothermal reduction of SnO$_2$ produces vapor consisting of Sn, O and Ag atoms. At the initial stage, a fraction of the evaporated Sn atoms gets oxidized in the atmosphere containing O atoms leading to

the formation of a large number of SnO_2 nanoparticles. These SnO_2 nanoparticles collide with each other and combine by OA in vapour phase to form SnO_2 microcrystals as shown in **Fig. 5 (a)**. A fraction of the evaporated Sn atoms gets deposited onto the substrates as Sn nanoparticles. This can be seen from XRD pattern shown in **Fig. 2**. In addition, few Sn-Ag nanodroplets form due to alloying of Sn nanoparticles with very small concentration of Ag atoms. These few Sn-Ag nanodroplets formed on the substrate at higher temperature leads to the formation of very small number of SnO_2 nanowires by vapour-liquid-solid (VLS) growth mechanism. In an earlier work **[37]** we have reported fabrication of SnO_2 nanotowers and interconnected nanowires by carbothermal evaporation using higher Ag concentrations of 5% and 10%, respectively. We have shown that the number density of SnO_2 nanowires increases with increase in Ag concentration. In the present case, very few nanowires are obtained at a low Ag concentration of 1% as can be seen from FESEM results shown in **Fig. 1 (a-b)**. At the initial stage of deposition, the SnO_2 microcrystals collide constantly with the substrate and adsorb onto the surface. After SnO_2 crystallites were deposited on the substrate, the subsequent crystallites deposit onto the adsorbed SnO_2 microcrystals. Because the adsorbed SnO_2 crystallites possess different shapes and orientations, the combination probability of the succeeding crystallites mainly depends on the surface energies and structure of the crystallites. Due to this a suitable structure of the microcrystals is critical for the inter-connected growth of SnO_2 microcrystals. However, our results shown in **Fig. 1** clearly show that no matter whether the succeeding SnO_2 crystallite is regular in shape or not, there will always be a suitable site for it to attach, and generally only the microcrystals with the same or similar shapes attach together. With more and more SnO_2 microcrystals attaching to the existing SnO_2 microcrystals one by one in the same way, 3D complex chain-like microstructures are formed as seen in **Fig. 1 (a-d)**. We have demonstrated that 3D complex chains of SnO_2 microcrystals can be easily fabricated by carbothermal reduction based vapor phase deposition via oriented attachment mechanism.

Conclusion

In summary, we report a simple carbothermal reduction based vapour deposition method for the fabrication of 3D complex chains of microcrystals of SnO_2. FESEM studies revealed the presence of 3D complex chains of SnO_2 microcrystals of varying size. The interconnected growth of SnO_2 microcrystals followed the oriented attachment mechanism resulting in the formation of 3D complex chains of microcrystals. PL studies revealed peaks at 361, 407, 438 and 465 nm. We believe that the fabricated 3D complex chains of SnO_2 microcrystals can find potential applications as building blocks of novel functional devices.

Reference

1. Wang, Y.; Jiang, X.; Xia, Y. *J. Am. Chem. Soc.* **2003**,*125*, 16176.
   DOI: 10.1021/ja037743f
2. Sakai, G.; Nam, S. B.; Miura, N.; Yamazoe, N. *Sen. Actuators B* **2001**, *77*, 116.
   DOI: 10.1016/S0925-4005(01)00682-7
3. Kolmakov, A.; Klenov, D. O.; Lilach, Y.; Stemmer, S.; Moskouits, M. *Nano Lett.* **2005**, *5*, 667.
   DOI: 10.1021/nl050082v
4. Kuang, Q.; Lao C.-S.; Li, Z.; Liu, Y.-Z.; Xie, Z.-X.; Zheng, L.-S. ; Wang, L. Z. *J. Phys. Chem. C* **2008**, *112*, 11539.
   DOI: 10.1021/jp802880c
5. Wu, S.S.; Cao, H.Q.; Yin, S.F.; Liu, X.W.; Zhang, X.R. *J. Phys. Chem. C* **2009**, *113*, 17893.
   DOI: 10.1021/jp9068762
6. Wang, W. W.; Zhu, Y .J.; Yang, L. X. *Adv. Funct. Mater.* **2007**, *17*, 59.
   DOI: 10.1002/adfm.200600431
7. Liu, Z.; Zhang, D.; Han, S.; Li. C.; Tang, T.; Jin, W.; Liu, X.; Lei, B.; Zhou, C. *Adv. Mater.* **2003**, *15*, 1754.
   DOI: 10.1002/adma.200305439
8. Zhu, J.; Lu, Z.; Aruna, S. T.; Aurbach, D.; Gedanken, A .*Chem. Mater.* **2000**, *12*, 2557.
   DOI: 10.1021/cm990683l
9. Dai, Z. R.; Pan, W.; Wang, Z. L. *J. Am. Chem. Soc.* **2002**, *124*, 8673.
   DOI: 10.1021/ja026262d
10. Zhang, L.; Yin, Y. *Sens. Actuators B: Chem.* **2013**, *185*, 594.
    DOI: 10.1016/j.snb.2013.05.068
11. Li, L. *Mat. Lett.* **2013**, *98*, 146.
    DOI: 10.1016/j.matlet.2013.02.038
12. Gu, F.; Wang, S.; Cao, H.; Li, C. *Nanotechnology* **2008**, *19*, 095708.
    DOI: 10.1088/0957-4484/19/9/095708
13. Trung, D. D.; Toan, N. V.; Tong P.V., Duy, N. V.; Hoa, N. D.; Hieu, N. V. *Ceramics Inter.* **2012**, *38*, 6557.
    DOI: 10.1016/j.ceramint.2012.05.039
14. Penn, R. L.; Banfield, J. F. *Science* **1998**, *281*, 969.
    DOI: 10.1126/science.281.5379.969
15. Banfield, J. F.; Welch, S. A.; Zhang, H.; Ebert, T. T.; Penn, R. L. *Science* **2000**, *289*, 751.
    DOI: 10.1126/science.289.5480.751
16. Penn, R. L.; Banfield, J. F. *Geochim. Cosmochim. Acta* **1999**, *63*,1549.
    DOI: 10.1016/S0016-7037(99)00037-X
17. Penn, R. L.; Oskam, G.; Strathmann, T. J.; Searson, P. C.; Stone, A. T.; Veblen, D. R. *J. Phys. Chem. B* **2001**, *105*, 2177.
    DOI: 10.1021/jp003570u
18. Zhang, H.; Banfield, J. F. *Chem. Mater.* **2002**, *14*, 4145.
    DOI: 10.1021/cm020072k
19. Zhang, H.; Banfield, J. F. *Nano Lett.* **2004**, *4*, 713.
    DOI: 10.1021/nl035238a
20. Tang, Z.; Kotov, N. A.; Giersig, M. *Science* **2002**, *297*, 237.
    DOI: 10.1126/science.1072086
21. Pacholski, C.; Kornowski, A.; Weller, H. *Angew. Chem. Int. Ed.* **2002**, *41*, 1188.
    DOI: 10.1002/1521-3773(20020402)41:7<1188::AID-ANIE1188>3.0.CO;2-5
22. Lee, J. H. E.; Riberio, C.; Longo, E.; Leite, E. R. *J. Phys. Chem. B* **2005**, *109*, 20842.
    DOI: 10.1021/jp0532115
23. Stroppa, D. G.; Montoro, L. A.; Beltran, A.; Conti, T. G.; Andres, J.; Leite, E. R.; Ramirez, A. J. *Chem. Commun.* **2011**, *47*, 3117.
    DOI: 10.1039/C0CC04570E
24. Zhuang, Z.; Zhang, J.; Haung, F.; Wang, Y.; Lin, Z. *Phys. Chem. Chem. Phys.* **2009**, *11*, 8516.
    DOI: 10.1039/B907967J
25. Cheng, B.; Samulski, E.T. *Chem. Commun.* **2004**, *8*, 986.
    DOI: 10.1039/B316435G
26. Houtepen, A. J.; Koole, R.; Vanmaekelbergh, D.; Meeldijk, J.; Hickey, S. G. *J. Am. Chem. Soc.* **2006**,*128*, 6792.
    DOI: 10.1021/ja061644v
27. Li, Z.; Xu, F.; Sun, X.; Zhang, W. *Cryst. Growth Design* **2008**, *8*, 805.
    DOI: 10.1021/cg060830+
28. Sangeetha, P.; Sasirekha, V.; Ramakrishnan, V. *J. Raman Spectrosc.* **2011**, 42, 1634.
    DOI: 10.1002/jrs.2919

29. Wang, X.; Fan, H.; Ren, P. *Colloid. Surf. A: Physicochem. Eng. Aspects* **2013**, 419, 140.
    DOI: 10.1016/j.colsurfa.2012.11.050
30. Peercy, P. S.; Morosin, B. *Phys. Rev. B* **1973**, 7, 2779.
    DOI: 10.1103/PhysRevB.7.2779
31. Sun, S. H.; Meng, G. W.; Zhang, G. X.; Gao, T.; Geng, B. Y.; Zhang, L. D.; Zuo, *Chem. Phys. Lett.* **2003**, 376, 103.
    DOI: 10.1016/S0009-2614(03)00965-5
32. Dieguez, A.; Romano- Rodriguez, A.; Vila, A.; Morante, J. R. *J. Appl. Phys.* **2001**, 90, 1550.
    DOI: 10.1063/1.1385573
33. Sangaletti, L.; Depero, L. E.; Allieri, B.; Pioselli, F.; Comini, E.; Sberveglieri, G.; Zocchi, M. *J. Mater. Res.* **1998**, 13, 2457.
    DOI:10.1557/JMR.1998.0343
34. Luo, S.; Fan, J.; Liu, W.; Zhang, M.; Song, Z.; Lin, C.; Wu, X.; Chu, P.K. *Nanotechnology* **2006**, *17*, 1695.
    DOI:10.1088/0957-4484/17/6/025
35. Pal, U.; Pal, M.; Zeferino, R.S. *J. Nanopart. Res.* **2012**,*14*, 969.
    DOI: 10.1007/s11051-012-0969-3
36. Kar, A.; Kundu, S.; Patra, A. *J. Phys. Chem. C* **2011**,*115*, 118.
    DOI: 10.1021/jp110313b
37. Bhardwaj, N.; Kuriakose, S.; Mohapatra, S. *J. Alloys Comp.* **2014**, *592*, 238.
    DOI: 10.1016/j.jallcom.2013.12.268